Computers and Geotechnics 63 (2015) 279–290

Contents lists available at ScienceDirect

Computers and Geotechnics

journal homepage: www.elsevier.com/locate/compgeo

Research Paper

Application of a Coupled Eulerian–Lagrangian approach on pile installation problems under partially drained conditions

Thorben Hamann [a,*], Gang Qiu [b], Jürgen Grabe [a]

[a] Hamburg University of Technology, Institute of Geotechnical Engineering and Construction Management, Harburger Schloßstraße 20, D-21079 Hamburg, Germany
[b] IMPaC Offshore Engineering, Hohe Bleichen 5, D-20354 Hamburg, Germany

ARTICLE INFO

Article history:
Received 5 December 2013
Received in revised form 18 August 2014
Accepted 12 October 2014
Available online 31 October 2014

Keywords:
Coupled Eulerian–Lagrangian
Consolidation
Large deformations
Pile installation
Two-phase material simulation
Fully saturated soil

ABSTRACT

A numerical technique for modeling the soil as a two-phase medium by means of a user material subroutine is presented. The approach is applied to a classical FE analysis in a Lagrangian formulation using an explicit time integration rule and to a Coupled Eulerian–Lagrangian approach. The application of these two approaches to the problem of pile jacking into fully saturated soil under partially drained conditions is investigated and compared to the solution obtained by use of an iterative equation solver. The influence of the installation process as well as the influence of the permeability on the surrounding soil is investigated.

1. Introduction

Offshore seabed or soil in harbor areas is normally fully saturated and can be regarded as a two-phase porous medium. Numerical methods can be a helpful tool for the analysis of the installation process of piles, spudcan foundations, pipelines or sheet pilings. For the analysis, fully coupled FE methods are usually applied to compute the fluid flow through a porous medium over a large time period in case of static or quasi-static loading conditions (e.g. a consolidation analysis). Since fluid flow is usually considered to be a slow process and long periods of time are investigated in an analysis, common FE codes like Abaqus use an iterative equation solver for this kind of analysis. In case of large FE models with relatively short response times as well as for the analysis of extremely discontinuous processes, an explicit equation solver is often preferred due to its computational efficiency [3]. But in common FE codes like Abaqus the use of an explicit equation solver is restricted for modeling only one-phase materials.

Considering the problem of pile installation under drained soil conditions different approaches related to the use of equation solver as well as the formulation in the spatial domain can be found in literature. An implicit integration scheme is applied to calculate the pile jacking process in Grabe and König [6], Sheng et al. [27] and Yi et al. [33]. The numerical results were validated by comparison with the measured pile resistance. However, it is essential to improve the robustness and accuracy of the numerical algorithms to simulate more realistic and complex features as for example piles under cyclic loading, piles with flat ends or piles in soils with excess pore pressure development [27]. Arbitrary Lagrangian Eulerian (ALE) methods [11,13] can be used to improve the robustness of the numerical simulations of pile installation [30] and footing problems [31]. Mahutka et al. [20] presented an ALE model to simulate the vibratory pile driving under cyclic loading using an explicit equation solver. An Eulerian method offered by the commercial package FEAT has been used by Dijkstra et al. [4] to investigate the change of soil conditions near the pile after pile installation. The pile was simulated with a flat end. A Coupled Eulerian Lagrangian (CEL) approach [1], which is based on an explicit time integration formulation, has been developed and implemented in the FE code Abaqus to deal with geotechnical problems involving large soil deformations. The CEL method has been applied by Qiu et al. [23] to simulate the jacking process of a pile into sand and the results were compared to results of a conventional explicit simulation. However, the discussed publications simulated the soil to be under drained conditions. The change of pore water pressure is not taken into account during the penetration of piles.

Accounting for the influence of pore water to the problem of pile installation, Qiu and Grabe [22] used the penalty approach and represented a numerical model using an explicit time integration rule

* Corresponding author.
E-mail address: thorben.hamann@tuhh.de (T. Hamann).

http://dx.doi.org/10.1016/j.compgeo.2014.10.006
0266-352X/

to simulate the cone penetration test in a saturated fine-grained soil. The soil is simulated to be under undrained conditions. Sabetamal et al. [25] presented a numerical method for modeling fully saturated soil under partially drained conditions and dynamic loading. Within this approach an implicit equation solver is used. The problem of rapid pile jacking as well as the installation of a torpedo anchor are modeled. Recently, meshfree methods are used to analyze the fully coupled hydro-mechanical behavior of saturated porous media [34,26]. By use of a solid and fluid velocity formulation (v–w formulation), Jassim et al. [15] extended the material point method to analyze coupled dynamic, two phase boundary value problems.

The problem of pile installation in fully saturated soil is an example of a large deformation problem, where extremely discontinuous processes in the soil have to be modeled and often large models with relatively short response times are computed. Hence, an explicit equation solver seems to be well suited for this kind of analysis. A numerical technique for modeling the soil as a two-phase medium by means of a user material subroutine is presented in this paper. By use of this technique a common one-phase analysis procedure can be extended to model fully saturated soil as a two-phase porous medium under partially drained conditions. A hypoplastic model is used to describe the behavior of the solid skeleton. The process of pile installation and the effect of consolidation is investigated. The application of this technique in a classical finite element analysis using a Lagrangian formulation with an explicit time integration rule as well as the application in the CEL method is studied. The solution as well as the computational effort of each method is compared to an analysis using an iterative equation solver.

2. Numerical method

Three different finite element analysis procedures are used to model the process of pile jacking into fully saturated soil. A classical finite element analysis in a Lagrangian formulation using an iterative equation solver provided by the finite element software code Abaqus/Standard [3]. The second approach (Abaqus/Explicit) is also a classical finite element analysis in a Lagrangian formulation, but uses an explicit time integration rule. The third approach (Abaqus/CEL) applies the Coupled Eulerian–Lagrangian method provided by Abaqus and uses an explicit time integration rule. The first procedure (Abaqus/Standard) allocates the numerical modeling of fully saturated soil by use of build-in features. The second and third approach, generally limited to a one-phase material, are extended by use of a user-subroutine for constitutive models to allow for the modeling of the soil as a two-phase material. This approach is described more in detail in the following. The numerical solutions of the three approaches are compared with each other to evaluate their application to coupled pore fluid diffusion and stress analysis of geotechnical boundary value problems. The first approach provided by Abaqus/Standard serves as reference.

2.1. Abaqus/Standard

The FE code Abaqus/Standard provides an analysis procedure for a coupled pore fluid diffusion and stress analysis of geotechnical boundary value problems limited to quasi-static loading conditions. The analysis procedure uses an iterative linear equation solver applying the newton method to solve the equilibrium equations [3]. Therefor, the simulation is broken into a certain number of time increments. By use of an iterative equation solver the approximate equilibrium of the system of equations is achieved iteratively at the end of each time increment until a given tolerance value is reached. The soil is considered as a multiphase medium. The fluid flow of up to two fluids through a porous medium can be modeled using the principle of effective stress. Fully saturated and partially saturated conditions can be considered. The FE mesh is attached to the solid phase. The fluid flows through the mesh. For the solid phase most of the implemented constitutive models, e.g. linear elastic model and Mohr–Coulomb model as well as user defined constitutive models such as hypoplasticity model, can be applied. To describe the fluid flow a continuity equation for the mass of the wetting fluid in a unit volume of the medium is used. Forchheimer's flow law (Eq. (1)) as well as a Darcy flow (Eq. (2)) as a special case of the Forchheimer's flow law can be applied. In the following only a Darcy flow is considered.

$$\boldsymbol{v}_{ws}(1+\beta\boldsymbol{v}_{ws}) = \frac{\kappa}{\mu_w}(-\nabla p_w + \rho_w \boldsymbol{b}) \tag{1}$$

$$\boldsymbol{v}_{ws} = \frac{\kappa}{\mu_w}(-\nabla p_w + \rho_w \boldsymbol{b}) \tag{2}$$

where $\boldsymbol{v}_{ws}$ is the fluid velocity relative to the solid skeleton, β is a permeability coefficient of Forcheimer's flow law, κ is the intrinsic permeability, μ_w is the dynamic viscosity, p_w is the pore pressure, ρ_w is the density of the fluid and $\boldsymbol{b}$ is the body force per unit mass (gravity).

2.2. Abaqus/Explicit

The explicit equation solver of Abaqus/Explicit generally solves the equation of motion without a damping term (Eq. (3)) at each node of the FE model [3]:

$$\boldsymbol{M}\boldsymbol{a}_s + \underbrace{\boldsymbol{K}\boldsymbol{u}_s}_{\boldsymbol{F}_{int}} = \boldsymbol{F}_{ext} \tag{3}$$

where $\boldsymbol{M}$ is the lumped mass matrix, $\boldsymbol{a}_s$ are the nodal accelerations, $\boldsymbol{K}$ is the stiffness matrix, $\boldsymbol{u}_s$ are the nodal displacements, $\boldsymbol{F}_{int}$ is the nodal internal force vector and $\boldsymbol{F}_{ext}$ is the nodal force vector due to an applied external load. The explicit equation solver uses an explicit central-difference integration rule for integration in the time domain. The solution of displacements $\boldsymbol{u}_s^{t_{i+1}}$ at the end of the current time increment Δt_i can be calculated using known values of acceleration $\boldsymbol{a}_s^{t_i}$ at the beginning of the current time increment and known values of velocity $\boldsymbol{v}_s^{t_{i-0.5}}$ at the midpoint of the previous time increment Δt_{i-1} (Eqs. (4) and (5)).

$$\boldsymbol{v}_s^{t_{i+0.5}} = \boldsymbol{v}_s^{t_{i-0.5}} + \frac{\Delta t_{i-1} + \Delta t_i}{2}\boldsymbol{a}_s^{t_i} \tag{4}$$

$$\boldsymbol{u}_s^{t_{i+1}} = \boldsymbol{u}_s^{t_i} + \Delta t_i \boldsymbol{v}_s^{t_{i+0.5}} \tag{5}$$

where $\boldsymbol{v}_s^{t_{i+0.5}}$ are the nodal velocities at the midpoint of the current time increment and $\boldsymbol{u}_s^{t_i}$ are the nodal displacements at the beginning of the current time increment. The nodal accelerations $\boldsymbol{a}_s^{t_{i+1}}$ at the end of the current time increment are calculated applying the equation of motion (Eq. (6)).

$$\boldsymbol{a}_s^{t_{i+1}} = \boldsymbol{M}^{-1}\left(\boldsymbol{F}_{ext}{}^{t_{i+1}} - \boldsymbol{F}_{int}^{t_{i+1}}\right) \tag{6}$$

Hence, no iteration is necessary. By using a lumped mass matrix the inversion of the mass matrix is trivial. Thus, the explicit dynamic procedure performs a large number of very small time increments efficiently. The central-difference operator is conditionally stable, if the time increments are less than a critical time increment Δt_{crit} (Eq. (7)). The critical time increment depends on the characteristic element length L_e and the dilatational wave speed c_d and is computed for each time step.

$$\Delta t_{crit} = \frac{L_e}{c_d} \tag{7}$$

To adopt this explicit analysis procedure to a dynamic fully coupled pore fluid diffusion and stress analysis for the special case of fully saturated conditions, the analysis procedure can be extended [8]. A u–p-formulation is used where the principle variables are the pore pressure p_w and the displacement of the solid phase u_s [35]. The equation of motion (Eq. (3)) is solved for the mixture of the solid and fluid phase carrying out a total stress analysis. The behavior of the fluid phase and the material behavior of the solid phase is implemented in the framework of a user subroutine for constitutive models. The user subroutine is called at each integration point of the model for each time increment. Strain increments are passed to the user subroutine and the updated total stress state is returned. Therefore, the user subroutine is separated into two parts: the first part for computation of the effective stress state and the second part for computation of the pore pressure. The effective stress state and the pore pressure are stored as internal state variables within the user subroutine.

The behavior of the solid skeleton is described with a hypoplastic constitutive model, see Section 2.4. To describe the behavior of the fluid phase within the user subroutine a continuity equation is applied (Eq. (8)):

$$\operatorname{div}\left(\underbrace{\frac{\kappa}{\mu_w}(-\nabla p_w - \rho_w \boldsymbol{a}_s + \rho_w \boldsymbol{b})}_{\text{Darcy's flow law}}\right) + \alpha_{biot}\boldsymbol{m}\dot{\boldsymbol{\varepsilon}}_s + \frac{\dot{p}_w}{Q} = 0 \tag{8}$$

with the Biot's constant α_{biot}:

$$\alpha_{biot} = 1 - \frac{K_T}{K_s} = 1 - \frac{\frac{E}{3-6\nu}}{K_s} \tag{9}$$

where $\boldsymbol{m}$ is the second order unit tensor, $\dot{\boldsymbol{\varepsilon}}_s$ is the strain rate of the solid skeleton, K_T is the bulk modulus of the solid skeleton, K_s is the bulk modulus of the solid particles, E is the Young's modulus of the solid skeleton and ν is the Poisson's ratio of the solid skeleton. The bulk modulus of the mixture of fluid and solid particles Q can be derived by Wood [32]:

$$\frac{1}{Q} = \frac{n}{K_w} + \frac{\alpha_{biot} - n}{K_s} \tag{10}$$

where n is the porosity and K_w is the bulk modulus of the fluid.

The fluid flow through the finite element mesh is modeled by Darcy's law (Eq. (2)). The relative acceleration $\boldsymbol{a}_{ws}$ of the fluid phase with respect to the solid phase is generally small and can be neglected [35]. If no high-frequency dynamic phenomena are considered, this assumption is usually acceptable [17]. Further, the solid particles are assumed to be compressible and isothermal conditions are considered. A derivation of the governing equations can be found in Zienkiewicz et al. [35]. Solving the mass balance equation of the water phase, the gradient of the pore pressure ∇p_w has to be computed, which is very expensive within the user-subroutine. Hence the similarity of Darcy's flow law (Eq. (11)) and heat conduction (Eq. (12)) is used, since Abaqus/Explicit provides a coupled temperature displacement analysis procedure.

$$\boldsymbol{v}_{ws} = \frac{\kappa}{\mu_w}\underbrace{(-\nabla p_w + \rho_w \boldsymbol{b})}_{-\nabla(\Delta p_w)} \tag{11}$$

$$\boldsymbol{f} = k(-\nabla\theta) \tag{12}$$

where $\boldsymbol{f}$ is the heat flux, k is the thermal conductivity and θ is the temperature. In order to adopt a temperature displacement analysis procedure for a coupled pore fluid and stress analysis, the temperature degree of freedom θ is coupled with the excess pore pressure Δp_w. Further, the thermal conductivity k and the specific heat c have to be adopted according to Eq. (12))

$$k = \frac{\kappa}{\mu_w} \tag{13}$$

$$c = \frac{1}{Q\rho} \tag{14}$$

with the density of the mixture:

$$\rho = (1-n)\rho_s + n\rho_w \tag{15}$$

where ρ_s is the density of the solid grains. Carrying out such an analysis the second term of the mass balance equation (Eq. (8)) meaning the change of pore pressure due to volumetric straining of the solid skeleton $\alpha_{biot}\boldsymbol{m}\dot{\boldsymbol{\varepsilon}}_s$ is computed within the user-subroutine and added to the temperature degree of freedom by use of inelastic heat generation. The first term of the mass balance equation meaning the diffusion of pore water is solved by heat conduction within the temperature displacement analysis procedure of Abaqus/Explicit. By use of the Abaqus/Explicit build-in feature of a coupled temperature displacement analysis procedure, such kind of analysis becomes very inexpensive compared to an analysis solving the whole mass balance equation within the user-subroutine. The main disadvantage is the neglection of the acceleration of the solid skeleton within Darcy's flow law. But as shown in Hamann and Grabe [8] this simplification has marginal influence on the solution, if quasi-static or slow processes are modeled.

2.3. Abaqus/CEL

Using a Lagrangian mesh to simulate the process of pile jacking into the soil, large deformations of the mesh which often result in problems due to the mesh distortion occur. The Coupled Eulerian–Lagrangian method is able to overcome the problem of mesh distortion [3]. The CEL method attempts to capture the advantages of both the Lagrangian and the Eulerian formulation.

A Lagrangian formulation is often used in a classical finite element analysis and is often applied in solid mechanics. In a Lagrangian formulation the material is fixed to a finite element. The material moves together with the nodes of the mesh during a simulation. Only a fluid in case of a coupled pore fluid diffusion and stress analysis can flow through the mesh. Thus, large deformations of the mesh can occur. The surface of a continuum is precisely defined by the surface of the Lagrangian mesh.

In an Eulerian formulation the nodes of a mesh are fixed in space. To allow for deformations during an analysis the material flows through the element mesh. The Eulerian material is tracked as it flows through the Eulerian mesh by computing its Eulerian volume fraction (EVF). The EVF is defined as the percentage of an Eulerian element which is filled with material. An EVF of zero means there is no material within the element and an EVF of one means that the element is completely filled with material. In contrast to the Lagrangian formulation, the surface of a continuum does not correspond to the element boundaries. The surface of the continuum has to be reconstructed using the EVF.

The Coupled Eulerian–Lagrangian method allows the interaction of a Lagrangian with an Eulerian continuum by using an Eulerian–Lagrangian contact algorithm based on a penalty contact method. A Lagrangian mesh can move through an Eulerian mesh without resistance. Contact occurs, if a Lagrangian element encounters an Eulerian element filled with material. The Eulerian time integration is realized applying the Lagrange-plus-remap formulation together with the central-difference operator described in Section 2.2. Each time increment consists of a first traditional Lagrangian phase (Section 2.2) followed by an Eulerian phase. In the Lagrangian phase the nodes are temporarily fixed to the material and the element deforms with the material. In the Eulerian phase a material flow is computed. The elements are tested for

significant deformations. These elements are remeshed and a material flow between neighboring elements is computed.

Generally, no pore fluid diffusion and stress analysis is implemented in the Abaqus/CEL method. The extension of this method for porous media allowing for a fluid flow is done by use of a user subroutine as described in Section 2.2. The pore fluid moves with the solid skeleton through the Eulerian mesh. Additionally, a fluid flow relative to the material flow due to a gradient of the pore pressure is possible.

2.4. Constitutive model

The pile is jacked into a coarse-grained sand with the soil properties of a so-called Mai-Liao sand from Cudmani [2]. The choice of an appropriate constitutive model to reproduce the behavior of the solid skeleton realistically is always a challenge. Soil is a strongly non-linear material. Linear elastic material behavior is only valid for small strains. During pile penetration the soil is compressed below the pile toe and pushed sideways. In case of dry soil conditions, areas with a compaction as well as areas with a loosening of the soil occur [9]. Since large deformations of the soil are considered in the following and the compaction process is important for the development of excess pore pressure, a hypoplastic constitutive model in the formulation of Gudehus [7] and Wolffersdorff [29] is used. The hypoplastic constitutive model is suitable to reproduce the non-linear and inelastic behavior of granular materials like sand realistically. Typical soil properties like dilatancy and contractancy, the dependency of the stiffness on the stress state and void ratio as well as different stiffnesses for loading and unloading can be described. An extension of intergranular strain proposed by Niemunis and Herle [21] allows to account for accumulation effects and hysteretic behavior in case of cyclic loading as well as the small strain behavior of soil. The constitutive model is rate independent in a rate-type formulation defined by the tensorial function, see Eq. (16):

$$\overset{\circ}{\mathbf{T}} = \mathcal{M}(\mathbf{T}, e, \boldsymbol{\delta}) : \mathbf{D} \tag{16}$$

where $\overset{\circ}{\mathbf{T}}$ is the objective Jaumann stress rate, $\mathcal{M}$ is a fourth order tensor, $\mathbf{T}$ is the current Cauchy stress, e is the void ratio, δ is the intergranular strain and $\mathbf{D}$ is the strain rate. The hypoplastic material parameters of the Mai-Liao sand are given in Table 1. Fig. 1 shows the results of element tests for Mai-Liao sand. It can be seen from Fig. 1(a), that the stiffness of the soil depends on the stress level. An secant modulus from oedometer tests E_{oed} about 2.3–3.9 MPa can be determined for loose Mai-Liao sand under a vertical stress from 50 kPa to 100 kPa. From the triaxial tests, it can be seen that the sand has a much lower shear strength under undrained conditions than it has under drained conditions (Fig. 1(b)).

Table 1
Hypoplastic material parameters for Mai-Liao sand [2].

Parameter	Value Mai Liao	Description
φ_c	31.5	Critical state friction angle (°)
h_s	32	Granular hardness (MN/m^2)
n	0.32	Exponent
e_{d0}	0.57	Minimum void ratio at zero pressure
e_{c0}	1.04	Critical void ratio at zero pressure
e_{i0}	1.20	Maximum void ratio at zero pressure
α	0.40	Exponent
β	1.00	Exponent
R	1×10^{-4}	Maximum value of intergranular strain
m_R	5.00	Stiffness ratio at a change of direction of 180°
m_T	2.00	Stiffness ratio at a change of direction of 90°
β_R	0.50	Exponent
χ	6.00	Exponent

3. Numerical model

The penetration of a circular pile with a diameter of $D = 30$ cm into fully saturated granular soil is investigated. Compared to a real piling problem the numerical model is simplified as described in the following. The influence of the pile jacking on the surrounding soil (e.g. effective stress state, void ratio and pore pressure) is analyzed. The results of the Lagragian approach using an explicit time integration scheme and of the CEL method are compared to the Lagrangian approach using an iterative equation solver.

3.1. Geometry and mesh

Two different finite element models are applied for comparison of the three approaches proposed before. An axisymmetric model is used to reduce computational costs in both the implicit and explicit analysis procedures using the Lagrangian approach. A three dimensional model is used for the CEL method, since this method is only available in a three dimensional formulation. The element size and the distribution of the element size is approximately the same in both models.

The axisymmetric model is shown in Fig. 2. The pile is modeled as a rigid body such that it does not experience any deformation during the simulation. Applying this simplification, it can be assumed that the influence on the solution of the problem would be small due to the much higher stiffness of a real pile (e.g. concrete) compared to the stiffness of soil. To avoid a distortion of the finite element mesh at the beginning of the penetration, the pile is modeled 50 cm pre-installed into the soil. Allowing for a penetration of the pile into the finite element mesh without distorting the mesh a so-called zipper-technique is applied. This technique was developed by Mabsout and Tassoulas [19] and can be described as follows: At the axis of symmetry, a vertical line through the mesh with a diameter of $D = 1$ mm is cut to provide a given shear band to be opened during pile penetration. To avoid closure of this cut, it is supported by a rigid tube which is in frictionless contact with the soil. During the penetration process the pile slides over the rigid tube, separates the soil from the tube and pushes the soil sideways. The numerical model is discretized in space with 4-noded linear quad-elements with reduced integration. The numerical model consists of 2422 nodes and 2317 elements. Loukidis and Salgado [18] suggest a very fine mesh with an element size of approximately $10D_{50}$ (element size of 2.0 mm) at the contact surface, if the shear band is located in the soil right beside the pile shaft (e.g. bored concrete piles with a rough surface). In the analysis performed within this paper the surface of the pile is assumed to be smooth such that the shear band between pile and soil is located in the contact surface. Thus, a larger element size compared to the element size recommended by Loukidis and Salgado [18] is chosen. The element size is 4.0 cm at the contact surface between pile and soil and 80.0 cm at the outer boundary of the model. The water level is defined at the ground level of the soil body. The sideways and bottom boundary are fixed in normal direction. The sideways boundary is defined to be permeable and the bottom boundary to be impermeable. A hydrostatic pore pressure distribution and a K_0-state according to Jaky [14] with $K_0 = 1 - \sin\varphi'$ and $\varphi' = 30°$ is assumed. The behavior of the solid skeleton is modeled with the hypoplastic constitutive model described in Section 2.4 with the parameters of Mai-Liao sand, see Table 1. Additional parameters for modeling the soil as a two-phase material are given in Table 2. The penetration process of the pile is modeled displacement-controlled with a penetration velocity of $v = 1$ m/s.

The three-dimensional model applying the CEL method is shown in Fig. 3. Using the axisymmetry of the problem only a

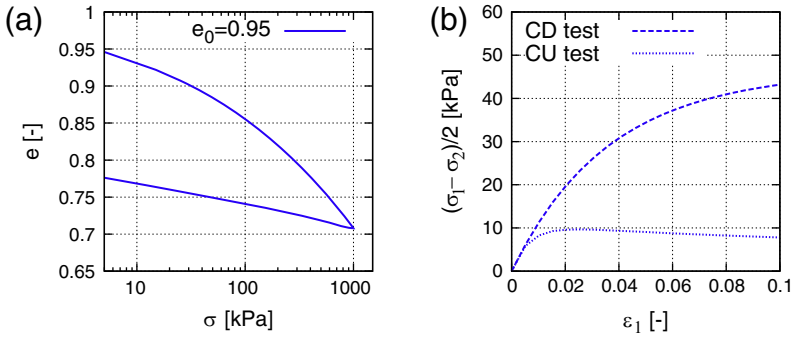

Fig. 1. Numerical simulation of element tests for Mai-Liao sand: (a) oedometric test and (b) triaxial test with initial radial pressure $\sigma_2^0 = \sigma_3^0 = 50$ kPa; $e_0 = 0.95$.

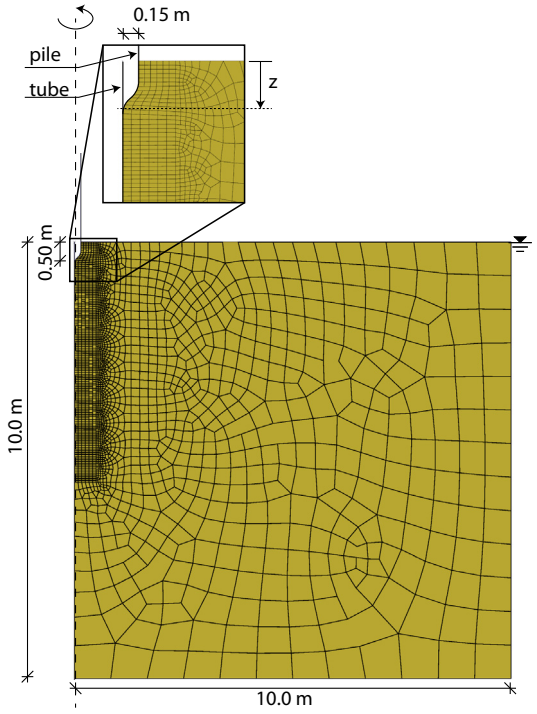

Fig. 2. Geometry and Lagrangian mesh of the axisymmetric model for simulation of the pile jacking into fully saturated sand.

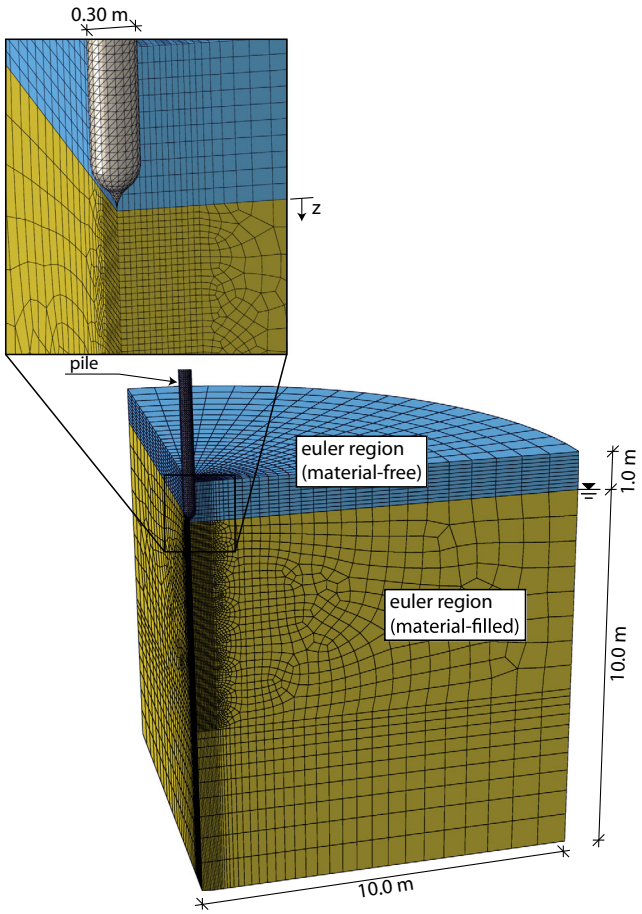

Fig. 3. Geometry and Eulerian mesh of the three-dimensional model for simulation of pile jacking into fully saturated sand.

Table 2
Additional parameters for modeling the soil as a two-phase material.

Parameter	Value	Description
ρ_s	2.65×10^3	Density of solid grains (kg/m^3)
ρ_w	1.0×10^3	Density of water (kg/m^3)
K_s	1.0×10^{15}	Bulk modulus of solid grains (kN/m^2)
K_w	2.0×10^6	Bulk modulus of water (kN/m^2)
k_s	1.0×10^{-4}	Hydraulic conductivity of solid (m/s)

quarter of a cylindrical soil body is modeled. The pile is modeled as a rigid body according to the axisymmetric model. At the beginning of the simulation, the pile is located at the ground level, no pre-installation is necessary, since the problem of mesh distortion is overcome by use of this method. The soil body is discretized in space using 8-noded linear brick elements with reduced integration. The model consists of 25,518 Eulerian elements and 39,890 nodes. The first two meter of the continuum are modeled without material at the beginning of the analysis. Thus, a material flow into this area during the penetration process of the pile is possible. Initial conditions, material parameters and boundary conditions are defined in accordance with the axisymmetric model.

3.2. Contact

The contact between the pile and the soil is modeled by a surface-to-surface contact algorithm in case of an axisymmetric simulation and by a general contact algorithm in case of a CEL simulation. In case of the surface-to-surface contact algorithm a master–slave-principle is applied, where the non-deformable pile represents the master surface and the soil represents the slave surface. A hard pressure–overclosure relationship with a penalty approach is used [3]. In order to decrease the problem of mesh

distortion in the contact surface, the surface of the pile is assumed to be smooth. Thus, the contact behavior in tangential direction is simplified as no friction is defined. This simplification will have an influence on the solution of the problem. But performing such a simulation it can be observed that the sand tends to liquefy with strongly reduced effective radial stresses at the contact surface during the penetration process. Thus, the effect of this simplification on the solution of the problem can be expected to be present but small.

4. Results

4.1. Verification

In Fig. 4 the distribution of the effective radial stress, the excess pore pressure and the void ratio after 5 m of pile jacking is shown for the three approaches. During pile penetration, the soil is pushed sidewards by the pile and the total radial stress increases. Due to the high bulk modulus of the pore water compared to the solid skeleton, excess pore pressure develops in the near-field around the pile. As a result of the excess pore pressure in the near-field, the effective stress decreases strongly. Below the pile tip very high excess pore pressure developed due to the high loading caused by the pile penetration. Regarding the void ratio it can be observed that the soil is densified in the very near-field around the pile. In case of partially drained conditions soil densification is a time-dependent process, since it depends on the consolidation of the soil. For the investigated case (pile penetration within a time-period of 5 s and a hydraulic conductivity of $k_s = 10^{-4}$ m/s) only a marginal densification of the soil from an initial relative density of $I_D = 0.2$ to $I_D = 0.22$ occurs. The relative desity I_D is defined as:

$$I_D = \frac{e_{max} - e}{e_{max} - e_{min}} \tag{17}$$

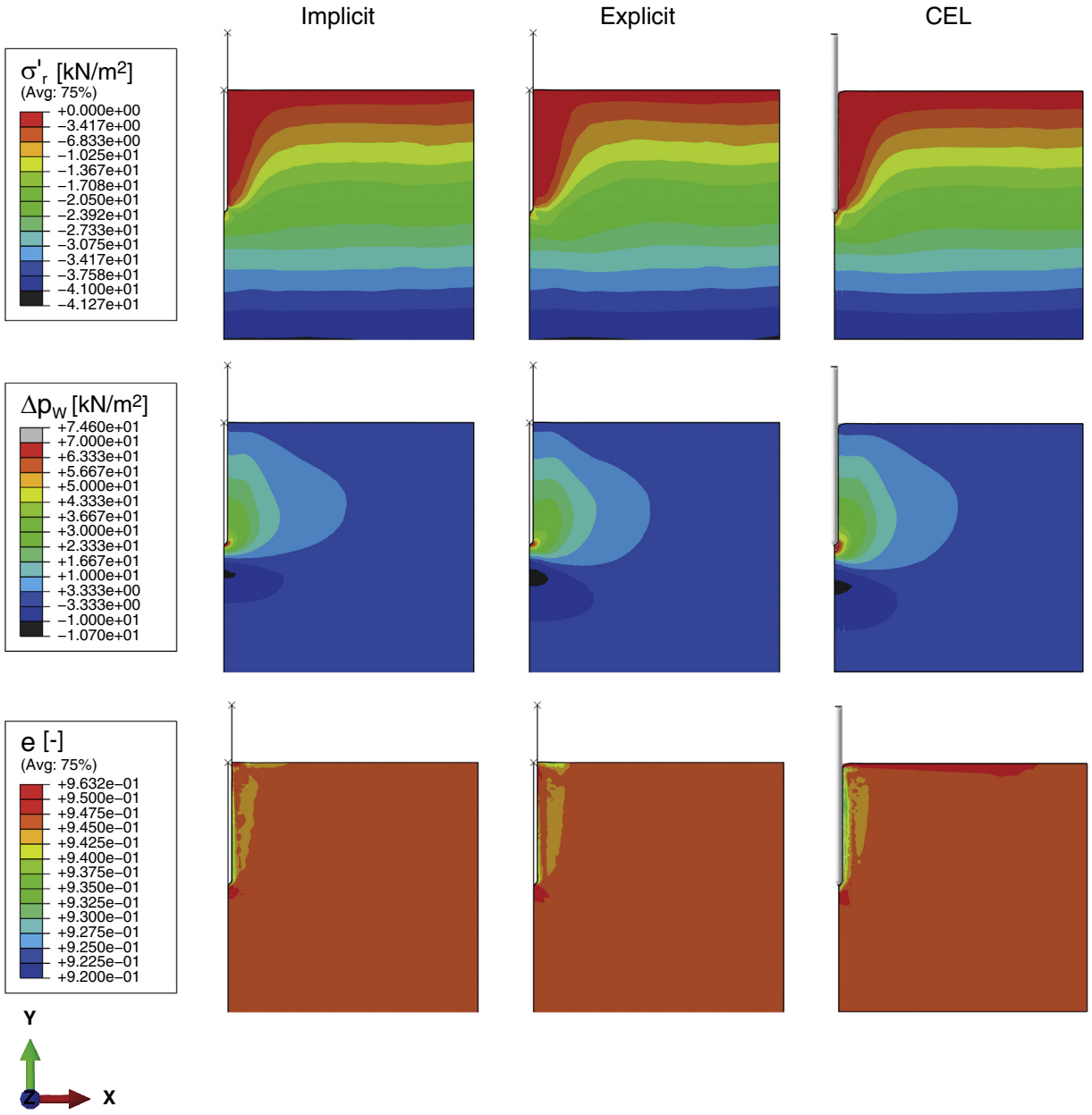

Fig. 4. Distribution of the effective radial stress σ'_r, the excess pore water pressure Δp_w and the void ratio e after 5 m of pile jacking into loose Mai-Liao sand ($I_D = 0.2$); comparison of implicit, explicit Lagrangian and CEL method.

in which e_{min} and e_{max} are the minimum and maximum void ratio obtained in the laboratory. The hypoplastic parameters e_{d0} and e_{c0} correspond to the e_{min} and e_{max} from index tests [10]:

$$e_{d0} = e_{max} \tag{18}$$

$$e_{c0} = e_{min} \tag{19}$$

The relative density can be obtained from Eq. (17) as:

$$I_D = \frac{e_{c0} - e}{e_{c0} - e_{d0}} \tag{20}$$

Since the excess pore pressure is not dissipated completely at the end of simulation, a further densification with ongoing simulation time can be expected.

To get a quantitatively more detailed comparison of the three applied analysis procedures, the distribution of the pore water pressure, the effective radial stress and the void ratio along a horizontal path at a depth of 2 m and 4 m for different penetration depths of the pile are depicted in Figs. 5 and 6. The pore water pressure and effective radial stress distribution of the explicit Lagrangian and the CEL simulation show a good agreement regarding the reference solution. The explicit procedures show the tendency to overestimate the pore pressure and the reduction of the effective stress marginally.

Regarding the pore water pressure distribution, a strong increase up to a distance of approximately 10 times the pile diameter at a depth of 2 m and approximately 15 times the pile diameter at a depth of 4 m can be observed after the pile tip has past. This phenomenon is caused by the radial compression of the solid skeleton and the flow resistance of the water through the solid skeleton, since partially drained conditions are defined. At the end of pile penetration, the maximum pore water pressure at the pile shaft has decreased already slightly due to consolidation. Thus, the pore water pressure rises slightly with increasing distance to the pile.

Regarding the effective radial stress, a decrease compared to the initial state up to a distance of approximately 5 times the pile diameter at a depth of 2 m and approximately 7 times the pile diameter at a depth of 4 m can be observed after the pile tip has past. This behavior is the result of the strong increase of the pore water pressure in this area. In a greater distance to the pile, the effective stress increases marginal. In the very near-field at the pile shaft the effective stress decreases below 3 kN/m^2, thus the soil shows the tendency to liquefy in this area. Hence, even if shaft friction would be specified, the influence of it seems to be of minor significance. At the end of pile penetration, the area with a decrease of the effective stress increases as a result of the expansion of the pore water pressure with ongoing simulation time.

The void ratio distribution of the two explicit procedures qualitatively shows the same behavior as the reference solution. A quantitative comparison indicates some differences concerning the curve progression. But it has to be taken into account that the change in void ratio is only within a very small range with a maximum change from $e = 0.946$ to 0.937. After the pile tip has past, a decrease of the void ratio up to a distance of approximately 3 times the pile diameter can be observed. At the end of pile penetration this area increases slightly to approximately 4 times the pile diameter due to consolidation.

Finally, the comparison of the three analysis procedures show that the solution of the explicit Lagrangian and the explicit CEL method fit quite well with the solution of the implicit Lagrangian procedure. There are marginal deviations to the solution of an implicit analysis to be expected. Applying an explicit analysis procedures a slight overestimation of the pore water pressure distribution arises. However, keeping in mind the advantages of the explicit procedures, these analysis procedures are a good alternative for the simulation of problems considering large deformations under partially drained conditions with a short duration.

4.2. Effect of partial drainage

In this section, the effect of partial drainage during the pile installation process in loose sand is investigated. Fig. 7 shows the results from ideal undrained, partially drained ($k_s = 1 \times 10^{-4}$ m/s) and ideal drained analysis by using the CEL method, when the tip of the pile is at a depth of 5 m. In the undrained analysis the effective radial stress σ'_r is reduced to near zero on the pile shaft and under the pile tip as well. However, concerning drained conditions the effective radial stress σ'_r on the pile shaft and under the pile tip is clearly increased due to the pile installation. In the partially drained analysis, the effective radial stress σ'_r on the pile shaft is reduced to almost zero, whereas the reduction of the stresses under the pile tip is not very dramatic. In the undrained analysis, the water is regarded to be nearly incompressible. The penetration of the pile leads to a significant change of the excess pore pressure Δp_w. It results in the reduction of the effective stress in the near-field of pile. The excess pore pressure Δp_w in the partially drained analysis is smaller than the value in the undrained analysis in the near-field of the pile due to consolidation. In the drained analysis

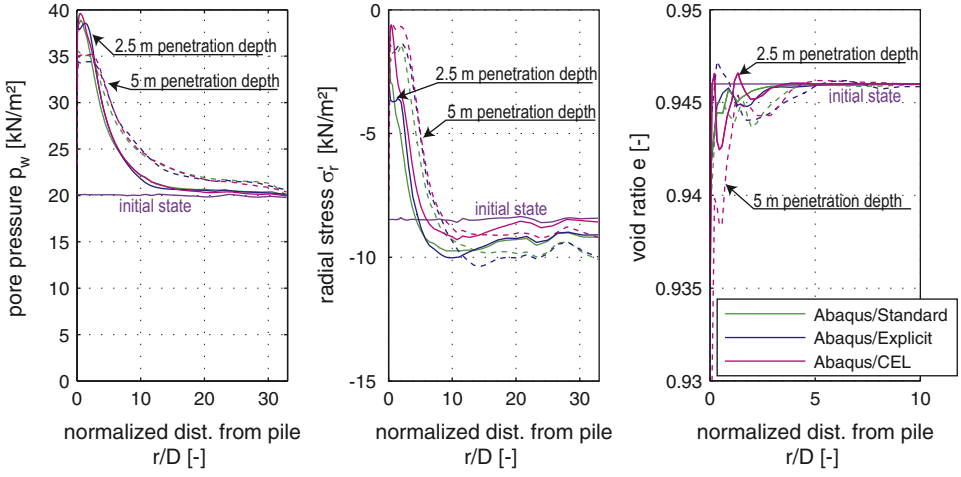

Fig. 5. Distribution of the pore water pressure, the effective radial stress and the void ratio at a depth of 2 m after 2.5 m (solid line) and 5 m (dashed line) of pile jacking into loose Mai-Liao sand ($I_D = 0.2$); r is the distance to pile shaft; D is the pile diameter.

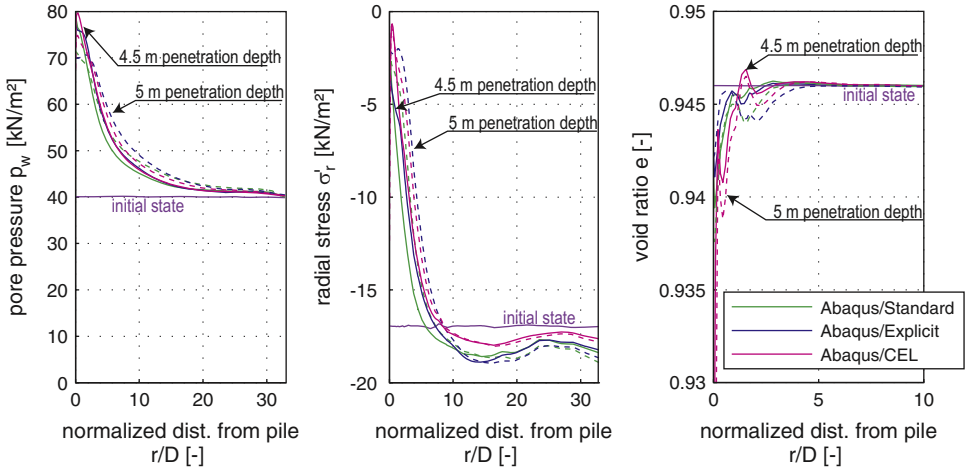

Fig. 6. Distribution of the pore water pressure, the effective radial stress and the void ratio at a depth of 4 m after 4.5 m (solid line) and 5 m (dashed line) of pile jacking into loose Mai-Liao sand ($I_D = 0.2$); r is the distance to pile shaft; D is the pile diameter.

the change of the pore pressure is ignored, therefore the excess pore pressure Δp_w is equal to zero throughout the whole penetration process. Concerning soil densification, the volume of the soil does not change in the undrained analysis, therefore the void ratio e remains constant. No compaction or loosening of the sand can be observed. In the drained analysis, the loose soil is clearly compacted in the near-field of the pile. Concerning an partially drained analysis, a slight compaction of the loose soil occurs in the near-field around the pile, since soil compaction depends on the consolidation of the soil.

4.3. Consolidation effect

With the objective to study the consolidation effect applying the proposed approach, a parametric study is performed. The two-dimensional model applying a Lagrangian formulation and an explicit time integration rule is used for this purpose. Within the parametric study no real piling problem is modeled. In the first study the pile is pushed at a high rate of penetration velocity of $v = 1$ m/s into the sand to achieve an adequate computational time for such kind of simulation. To study the effect of consolidation the values of hydraulic conductivity are varied in a range, where some values are unrealistically for a real sand. A correlation between grain size distribution or void ratio and the hydraulic conductivity is neglected. Another aspect to be kept in mind is that inertia effects will probably arise for the simulation with high penetration velocity. The penetration velocity of $v = 1$ m/s used in this study is relative low and the inertia effect can be ignored [28]. In the second study the effect of the rate of penetration velocity is investigated at a hydraulic conductivity of $k_s = 1 \times 10^{-4}$ m/s.

The vertical resistance of the pile according to the penetration depth is shown in Fig. 8(a) for different hydraulic conductivities of the soil. In case of simulating the process of pile penetration into loose Mai-Liao sand with a penetration velocity of $v = 1$ m/s the use of a hydraulic conductivity of $k_s \leqslant 1 \times 10^{-4}$ m/s shows the same results as an undrained simulation. The effect of consolidation during the penetration process becomes obvious for a hydraulic conductivity of $k_s \geqslant 1 \times 10^{-3}$ m/s.

Furthermore, the influence of the hydraulic conductivity on the behavior of the soil is shown for the distribution of the pore pressure, the effective radial stress and the void ratio along a horizontal path at a depth of 2 m and 4 m in Figs. 9 and 10. In accordance to the results regarding the vertical pile resistance the use of a hydraulic conductivity of $k_s \leqslant 1 \times 10^{-4}$ m/s shows approximately the same results as an undrained simulation. As expected a lower hydraulic conductivity of the soil results in a higher excess pore pressure and a stronger reduction of the effective stress in the near-field around the pile. Concerning the void ratio a densification up to a distance from the pile of $8D$ at a depth of 2 m and $6D$ at a depth of 4 m are calculated in case of a hydraulic conductivity of $k_s \geqslant 1 \times 10^{-3}$ m/s.

Assuming a slower more realistic penetration velocity, the simulation time for penetrating the pile into the soil up to a depth of 5 m increases. Further, inertia effects become less important. The effect of penetration velocity can be seen in Fig. 8(b). Assuming a penetration velocity of $v = 1$ m/s, the vertical resistance of the pile is the same compared to the case of undrained conditions, as already observed in Fig. 8(a). By reduction of the penetration velocity to $v \leqslant 0.25$ m/s the effect of penetration velocity becomes obvious as a result of consolidation and inertia effects.

According to Finnie and Randolph [5], the resistance of a penetrometer during the penetration into fully saturated soil under partially drained conditions can be described as a function of the normalized velocity V

$$V = \frac{vD}{c_v} \tag{21}$$

where v is the penetration velocity, D is the diameter of the penetrometer and c_v is the coefficient of the consolidation of the soil. Finnie and Randolph [5] suggested that the drained and undrained limits for V are around 0.01 and 30 respectively. The tests carried out by House et al. [12] with a cylindrical T-bar penetrometer suggest narrower limits of 0.1 and 10.

The average applied stress q_t is defined as:

$$q_t = \frac{R_v}{A} \tag{22}$$

where R_v is the total vertical resistance of the pile tip and A is the area of the pile cross section with $A = \pi/4D^2$. In case of a drained analysis only the effective stress is calculated, while the pore pressure is not taken into consideration. Therefore, the average applied stress for the drained analyses is defined as

$$q_t = q'_t + z\gamma_w \tag{23}$$

where q'_t is the average applied effective stress obtained from the drained analysis. The penetration depth z is defined as the distance from pile tip to the surface of the soil as indicated in Fig. 2.

Before comparing of the numerical results with experimental tests the mesh dependency of the numerical result is investigated

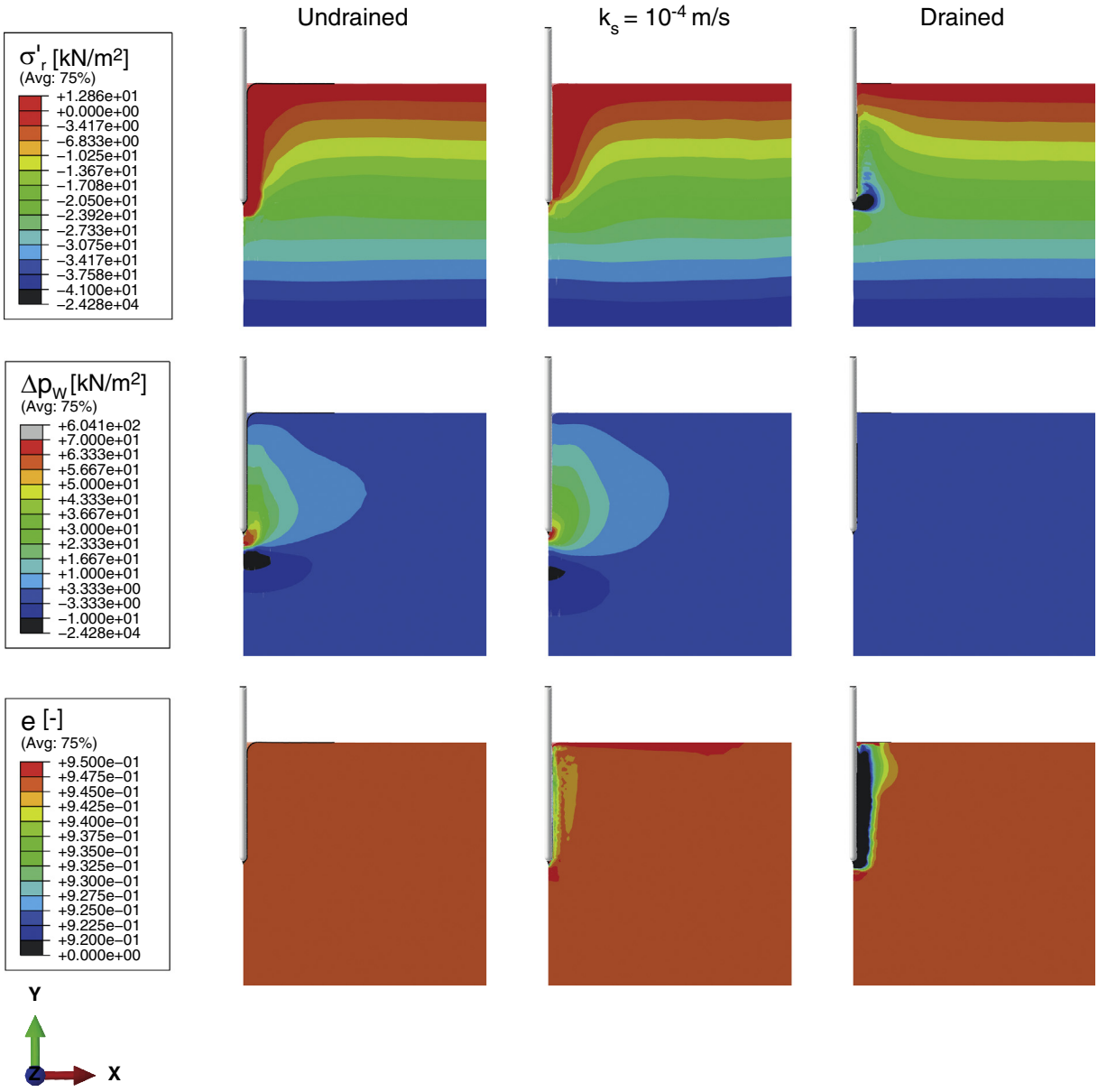

Fig. 7. Distribution of the effective radial stress σ'_r, the excess pore pressure Δp_w and the void ratio e after 5 m of pile jacking into loose Mai-Liao sand ($I_D = 0.2$) using CEL method.

in Fig. 11. The coarse mesh has an element size of 6 cm in height and 10 cm in width right at the pile shaft. Concerning the medium fine mesh, representing the mesh used in the studies before, the element size in the near-field around the pile is reduced to 4 cm in height and 8 cm in width at the pile shaft. The fine mesh has an element size of 2 cm in height and 4.5 cm in width at the pile shaft. The calculated vertical reaction force shows a slight influence of the element size in the near-field around the pile. For comparison with the experimental data the medium fine mesh is used.

The correlation between the normalized velocity V and the average applied stress q_t from the numerical results for loose Mai-Liao sand has been shown in Fig. 12. The result is compared with other results from experiments as well as numerical simulations. It can be seen from Fig. 12, that Mai-Liao sand shows a similar trend as the calcareous sand used by Finnie and Randolph [5]. The progression of the curves and especially the relation of q_t/q_{ref} in case of drained conditions is quantitatively not identical to the results of Finnie and Randolph [5], since another sand with different properties is used. But it can be shown, that the effect of consolidation observed in real penetration tests can be reproduced by application of this approach. A hyperbolic function with the form

$$\frac{q_t}{q_{ref}} = 1 + \frac{b}{1 + cV^m} \tag{24}$$

has been inferred by Randolph and Hope [24] for the backbone curve. q_{ref} is the reference (undrained) cone resistance [33]. The results for Mai-Liao sand can be fitted by

$$\frac{q_t}{q_{ref}} = 1 + \frac{1.63}{1 + 8.1V^{1.3}} \tag{25}$$

The effect of penetration rate on cone penetration resistance in saturated clayey soils has been studied by Kim et al. [16]. According to Yi et al. [33] the factor b in Eq. (24) depends significantly on the soil stiffness. For a given modulus ratio $G/p' = 35$, the numerical results of Yi et al. [33] can be fitted by

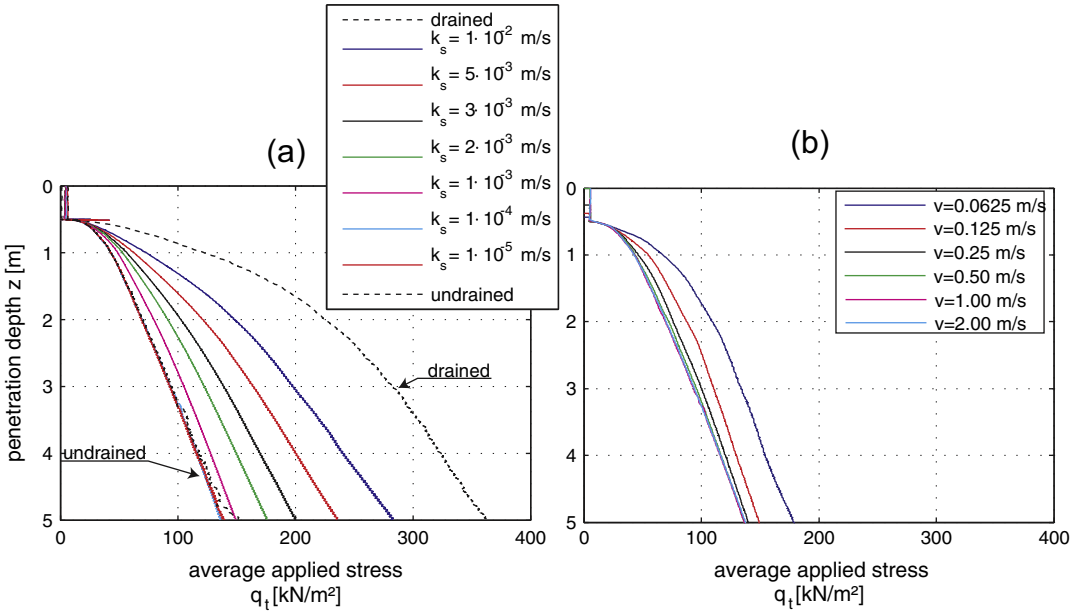

Fig. 8. Vertical reaction force during pile jacking into loose Mai-Liao sand ($I_D = 0.2$) (a) for different hydraulic conductivities k_s (penetration velocity $v = 1$ m/s) and (b) for different penetration velocities v (hydraulic conductivity $k_s = 1 \times 10^{-4}$ m/s).

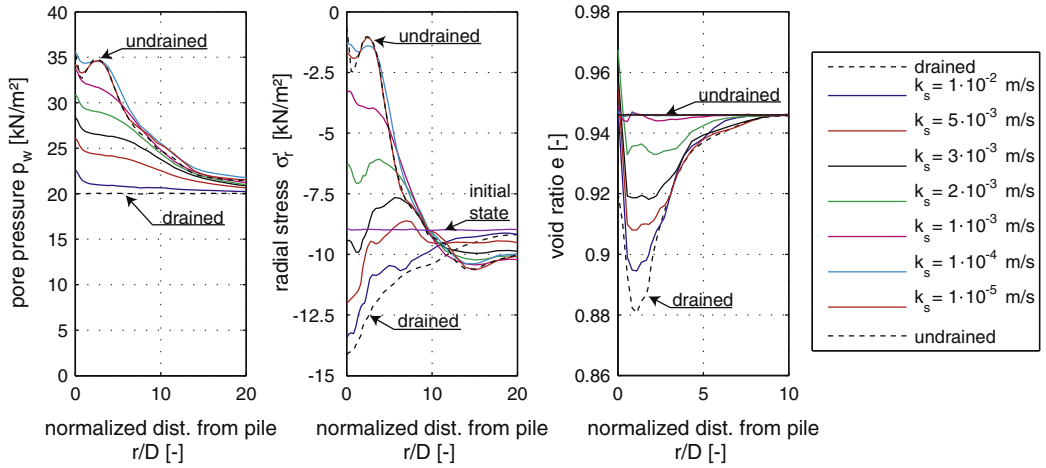

Fig. 9. Distribution of the pore pressure, the effective radial stress and the void ratio at a depth of 2 m after 5 m of pile jacking into loose Mai-Liao sand ($I_D = 0.2$) in dependence of hydraulic conductivity k_s; r is the distance to pile shaft; D is the pile diameter.

$$\frac{q_t}{q_{ref}} = 1 + \frac{1.1}{1 + 0.8V^{1.1}} \tag{26}$$

G is the soil shear modulus and p' is the mean effective normal stress. The soil in field tests from Kim et al. [16] has a higher modulus ratio $G/p' = 100$. The factor $b = 2.5$ has been estimated by Yi et al. [33] to fit the field test results from Kim et al. [16]. To overcome the uncertainties of in situ test results, calibration chamber penetration tests (P1 and P2) have been carried out by Kim et al. [16] and the results are shown in Fig. 12. It can be seen from all results, that the transition from partially drained to undrained condition occurs at $V \approx 10$. A narrow transition zone can be observed in the tests from Kim et al. [16] and numerical results from Yi et al. [33]. The transition from partially drained to fully drained can be observed at $V \approx 0.05$. A limit value of $V \approx 0.01$ can be obtained from present study, whereas a even lower value $V \approx 0.001$ can be obtained from centrifuge tests from Finnie and Randolph [5].

5. Parallelization

The parallelization of the numerical approach is investigated regarding the pile penetration problem. The calculations are carried out with up to 16 cores on the Linux cluster BOMBUS at the Hamburg University of Technology. The node used for the SpeedUp tests has 2 Intel Xeon Processors E5-2670 (8 cores each processor) and 64 GB RAM. In the calculations of pile jacking the soil is modeled as a three-dimensional Eulerian continuum consisting of 25,518 elements and 39,890 nodes and as an axisymmetric Lagrangian continuum consisting of 2317 elements and 2422 nodes. A domain-decomposition parallelization algorithm is used in all analyses using an MPI (Message Passing Interface) parallel execution. The SpeedUp-factor is defined as

$$\text{SpeedUp}(m) = \frac{t_1}{t_m} \tag{27}$$

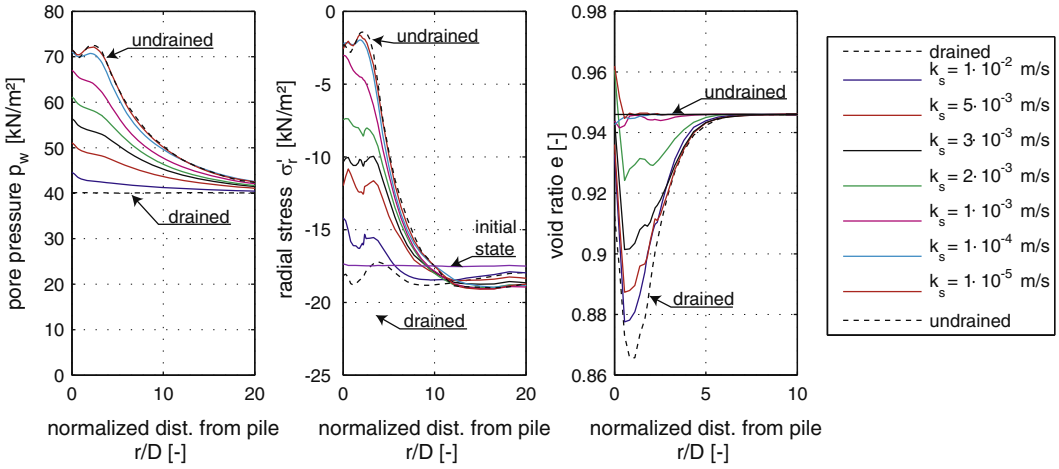

Fig. 10. Distribution of the pore pressure, the effective radial stress and the void ratio at a depth of 4 m after 5 m of pile jacking into loose Mai-Liao sand ($I_D = 0.2$) in dependence of hydraulic conductivity k_s; r is the distance to pile shaft; D is the pile diameter.

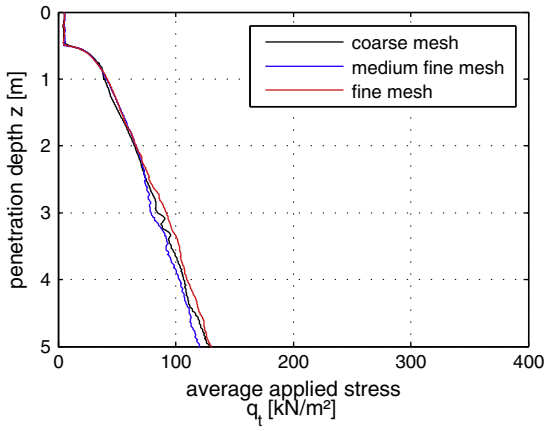

Fig. 11. Vertical reaction force during pile jacking into loose Mai-Liao sand ($I_D = 0.2$) with a hydraulic conductivity $k_s = 1 \times 10^{-4}$ m/s and a penetration velocity $v = 1$ m/s, variable the discretisation level.

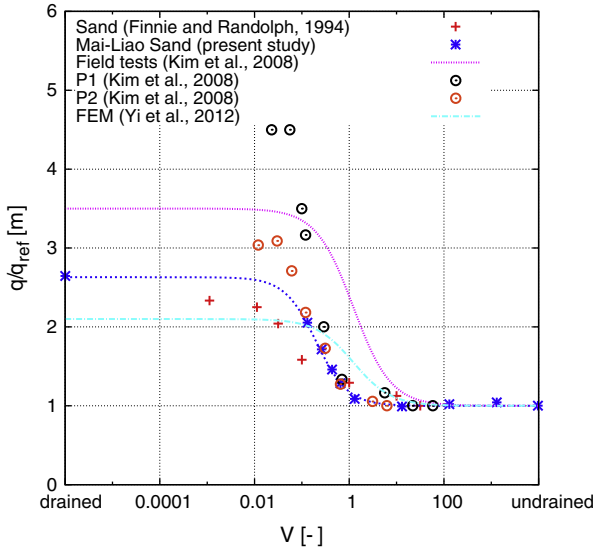

Fig. 12. Comparison of the numerical results with the experimental results from Finnie and Randolph [5].

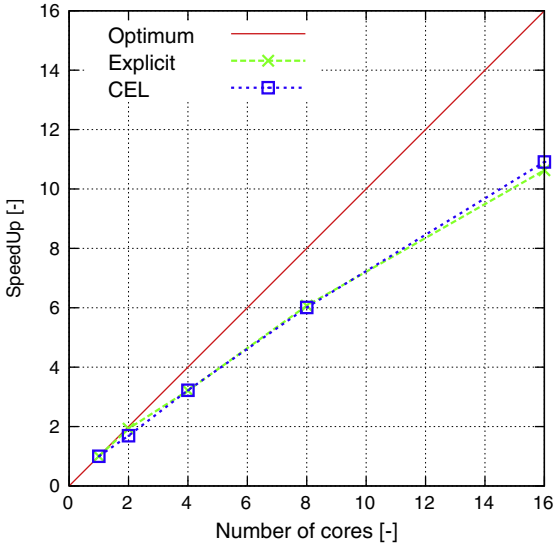

Fig. 13. SpeedUp factors for the simulations with the explicit Lagrangian and CEL method.

where t_1 is the execution time of the sequential algorithm, t_m is the execution time of the parallel algorithm with m cores.

It can be seen from Fig. 13 that the quality of the parallelization of the explicit Lagrangian method and the CEL approach is satisfactory. The SpeedUp-factor is about 11 using 16 cores. However, using the implicit approach show that no SpeedUp can be achieved by using multi-cores. The computational time of an implicit analysis is approximately 8 h, whereas the computational time of an explicit analysis is much shorter, approximately 2 h by using one core.

6. Conclusion

Numerical simulations of pile jacking into fully saturated soil have been carried out in this paper. The approach of modeling fully saturated soil in a dynamic analysis with an explicit time integration rule proposed by Hamann and Grabe [8] is used to solve such a geotechnical problem with large deformations under partially drained conditions.

Applying this approach on a dynamic explicit analysis using a Lagrangian formulation (Abaqus/Explicit) or on a Coupled Eulerian Lagrangian formulation (Abaqus/CEL), the results show only slight deviations to the results obtained by use of a quasi-static analysis with an iterative time integration rule (Abaqus/Standard). In particular, a slight overestimation of the excess pore pressure and of the reduction of the effective stress in the near-field of the pile can be observed. In return, a dynamic explicit analysis entails the advantages such as the higher computational efficiency in case of large models with short simulation times or for the analysis of extremely discontinuous processes. Especially the application of the approach on the CEL-method provides the possibility of modeling geotechnical problems with large deformations under partially drained conditions without the problem of mesh distortion.

By investigation of the problem of pile jacking in fully saturated soil, the effect of fully undrained, partially drained and fully drained conditions on the excess pore pressure, the effective stress and the void ratio can be shown. By decreasing the hydraulic conductivity k_s of the soil, higher excess pore pressure and a greater reduction of the effective stress in the near-field of the pile can be observed during the penetration process, as expected. The distance in which the pore pressure, the effective stress and the void ratio are effected by the process of pile jacking can be calculated. Depending on the hydraulic conductivity, an estimation is possible, if a soil with a given hydraulic conductivity will show a drained, a partially drained or an undrained behavior during loading. Furthermore, a correlation of the calculated vertical pile resistance with respect to the hydraulic conductivity and the penetration velocity fits well with experimental tests conducted by Finnie and Randolph [5]. A SpeedUp test on the problem of pile jacking shows that the quality of the parallelization of the explicit Lagrangian method and the CEL approach is satisfactory up to a simulation using 16 cores with a SpeedUp-factor of 11. Comparing the computational times of an implicit Lagrangian analysis with an explicit Lagrangian analysis using a single core, the advantage of the explicit method becomes obvious being nearly 4 times faster.

The approach proposed by Hamann and Grabe [8] to solve geotechnical problems with large deformations under partially drained conditions has been successfully applied together with the CEL method on the problem of pile jacking. The proposed numerical approach can also be used for the analysis of installation or extraction processes of spudcan foundations, suction buckets, pipelines or sheet pilings. Furthermore, the application of the approach on geotechnical problems with dynamic loading conditions will be investigated.

Acknowledgments

The present work has been funded by the German Research Foundation (DFG) in the framework of the research training group GRK 1096 "Ports for Container Ships of Future Generations". The authors thank the DFG for funding the work. Furthermore, the authors appreciate the academic use of the commercial program Abaqus.

References

[1] Benson DJ. Computational methods in Lagrangian and Eulerian hydrocodes. Comput Methods Appl Mech Eng 1992;99:235–394.
[2] Cudmani R. Statisch, alternierende und dynamische Penetration in nichtbindigen Böden. PhD thesis, Instituts für Bodenmechanik und Felsmechanik der Universität Karlsruhe; 2001.
[3] Dassault Systèmes. Abaqus User's Manual 2012. Dassault Systèmes; 2012.
[4] Dijkstra J, Broere W, van Tol AF. Eulerian simulation of the installation process of a displacement pile. In: Contemporary topics in situ testing, analysis, and reliability of foundations; 2008. p. 135–42.
[5] Finnie IMS, Randolph MF. Punch-through and liquefaction induced failure of shallow foundations on calcareous sediments. In: 17th international conference on the behaviour of offshore structures, Massachusetts, USA, Pergamon; 1994. p. 217–30.
[6] Grabe J, König F. Zur aushubbedingten Reduktion des Drucksondierwiderstandes. Bautechnik 2004;81(7):569–77.
[7] Gudehus G. A comprehensive constitutive equation for granular materials. Soils Found 1996;36(1):1–12.
[8] Hamann T, Grabe J. Simple dynamic approach for the numerical modeling of soil as a 2-phase-material. Geotechnik 2013;36(3):279–99.
[9] Henke S. Influence of pile installation on adjacent structures. Int J Numer Anal Methods Geomech 2010;34(11):1191–210.
[10] Herle I. Hypoplastizität und granulometrie einfacher korngerüste. PhD thesis, Instituts für Bodenmechanik und Felsmechanik der Universität Karlsruhe; 1997.
[11] Hirt CW, Amsden AA, Cook JL. An arbitrary Lagrangian–Eulerian computing method for all flow speeds. J Comput Phys 1974;14(3):227–53.
[12] House AR, Oliveira JRM, Randolph MF. Evaluating the coefficient of consolidation using penetration tests. Int J Phys Model Geotech 2001;1(3):17–26.
[13] Hu Y, Randolph MF. H-adaptive FE analysis of elasto-plastic non-homogeneous soil with large deformation. Comput Geotech 1998;23(1–2):61–83.
[14] Jaky J. Pressure in silos. In: Proc 2nd international conference on soil mechanics and foundation engineering, vol. 1; 1948. p. 103–7.
[15] Jassim I, Stolle D, Vermeer P. Two-phase dynamic analysis by material point method. Int J Numer Anal Methods Geomech 2012.
[16] Kim K, Prezzi M, Salgado R, Lee W. Effect of penetration rate on cone penetration resistance in saturated clayey soils. J Geotech Geoenviron Eng 2008;134(8):1142–53.
[17] Lewis R, Schrefler B. The finite element method in the static and dynamic deformation and consolidation of porous media. 2nd ed. John Wiley & Sons; 1998.
[18] Loukidis D, Salgado R. Analysis of the shaft resistance of non-displacement piles in sand. Géotechnique 2008;58(4):283–96.
[19] Mabsout ME, Tassoulas J. A finite element model for the simulation of pile driving. Int J Numer Anal Methods Eng 1994;37:257–78.
[20] Mahutka K-P, König F, Grabe J. Numerical modelling of pile jacking, driving and vibratory driving. In: Proceedings of international conference on numerical simulation of construction processes in geotechnical engineering for urban environment (NSC06); 2006. p. 235–46.
[21] Niemunis A, Herle I. Hypoplastic model for cohesionless soils with elastic strain range. Mech Cohes-Frict Mater 1997;2:279–99.
[22] Qiu G, Grabe J. Explicit modeling of cone and strip footing penetration under drained and undrained conditions using a visco-hypoplastic model. Geotechnik 2011;34(3):205–17.
[23] Qiu G, Henke S, Grabe J. Application of a coupled Eulerian–Lagrangian approach on geomechanical problems involving large deformations. Comput Geotech 2011;38(1):30–9.
[24] Randolph MF, Hope S. Effect of cone velocity on cone resistance and excess pore pressure. In: Pro 1st int symp on engineering practice and performance of soft deposits; 2004. p. 147–52.
[25] Sabetamal H, Nazem M, Carter J, Sloan S. Large deformation dynamic analysis of saturated porous media with applications to penetration problems. Comput Geotech 2014;55:117–31.
[26] Samimi S, Pak A. Three-dimensional simulation of fully coupled hydro-mechanical behavior of saturated porous media using Element Free Galerkin (EFG) method. Comput Geotech 2012;46(0):75–83.
[27] Sheng DC, Eigenbrod K, Wriggers P. Finite element analysis of pile installation using large-slip frictional contact. Comput Geotech 2005;32:17–26.
[28] Tho KK, Leung CF, Chow YK, Swaddiwudhipong S. Eulerian finite element technique for analysis of jack-up spudcan penetration. Int J Geomech 2012;12(1):64–73.
[29] von Wolffersdorff P. A hypoplastic relation for granular materials with a predefined limit state surface. Mech Cohes-Frict Mater 1996;1:251–71.
[30] Walker J, Yu H. Adaptive finite element analysis of cone penetration in clay. Acta Geotech 2006;1(1):43–57.
[31] Wang D, Randolph MF, White DJ. A dynamic large deformation finite element method based on mesh regeneration. Comput Geotech 2013;54:192–201.
[32] Wood A. A textbook of sound. B. Bell and Sons; 1930.
[33] Yi JT, Goh SH, Lee FH, Randolph MF. A numerical study of cone penetration in fine-grained soils allowing for consolidation effects. Géotechnique 2012;62(8):707–19.
[34] Zhang H, Wang K, Chen Z. Material point method for dynamic analysis of saturated porous media under external contact/impact of solid bodies. Comput Methods Appl Mech Eng 2009;198(17–20):1456–72.
[35] Zienkiewicz O, Chan A, Pastor M, Schrefler B, Shiomi T. Computational geomechanics with special reference to earthquake engineering. John Wiley & Sons; 1999.